NASA TECHNICAL NOTE

NASA TN D-4644

NASA TN D-4644

COLD-WALL THERMAL-VACUUM, THERMAL DESIGN CHECK FOR FULLY INSULATED EXPERIMENT PACKAGES

by Charles Dan

Goddard Space Flight Center
Greenbelt, Md.

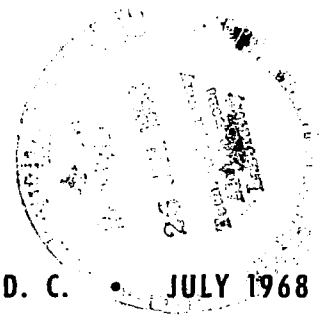

NATIONAL AERONAUTICS AND SPACE ADMINISTRATION • WASHINGTON, D. C. • JULY 1968

NASA TN D-4644

COLD-WALL THERMAL-VACUUM, THERMAL DESIGN CHECK FOR FULLY INSULATED EXPERIMENT PACKAGES

By Charles Dan

Goddard Space Flight Center
Greenbelt, Md.

NATIONAL AERONAUTICS AND SPACE ADMINISTRATION

For sale by the Clearinghouse for Federal Scientific and Technical Information
Springfield, Virginia 22151 – CFSTI price $3.00

ABSTRACT

Past procedure for testing the thermal balance of fully insulated experiment packages involved a solar-simulation test on the flight model as well as on the prototype. Experience gained during the OGO III spacecraft tests indicated that the solar simulation portion of the subsystem test could be eliminated for the flight model experiments without loss of confidence in the design. In the new procedure, validation of the flight model thermal balance is achieved, instead, by calculating the solar stabilization temperatures using data from a "cold-wall design check" and comparing the results with the solar-simulation test previously performed on the prototype model. Analytical development and procedures for employing this simplified approach are discussed.

CONTENTS

COLD-WALL THERMAL-VACUUM, THERMAL DESIGN CHECK FOR FULLY INSULATED EXPERIMENT PACKAGES

by
Charles Dan
Goddard Space Flight Center

INTRODUCTION

A simplified approach to the thermal-balance testing of fully insulated spacecraft experiments was developed at Goddard Space Flight Center during the Orbiting Geophysical Observatory III (OGO III) test program. Previous procedure had involved the running of a complete solar simulation test on the flight model as well as on the prototype experiment subsystems. The simplified method eliminates the solar-simulation test on the flight-model experiments, substituting a combined empirical-theoretical technique for validating the thermal balance.

The new technique is based on the fact that heat is transferred through the superinsulation and that the effectiveness of the insulation can be calculated for the flight-model experiments from data taken during the cold-wall, or eclipse-phase check. Because of its initial success in reducing time and effort while increasing confidence in the test the new technique was made an integral part of subsequent thermal-balance testing in the OGO program.

The possibilities of the new technique first came to light during the testing of OGO III. A thermal stabilization temperature achieved during the integrated, or "all-up system" test did not correlate with the value obtained during the prior subsystem test in the case of one package, namely, experiment package 1 (EP-1). The investigation of that anomaly led to the development of the new technique.

This report describes the temperature anomaly that led to the adoption of the new technique, the theory involved, and how the technique may be employed in future testing.

ANALYTICAL DEVELOPMENT

The test configuration is shown in Figure 1. It is seen that the fully insulated experiment is thermally isolated and mounted near the center of a thermal-vacuum chamber. Deep space is simulated by cryogenically cooled black shrouds that cover the chamber walls. A solar-simulation source is located so that the package may be irradiated on preselected surfaces.

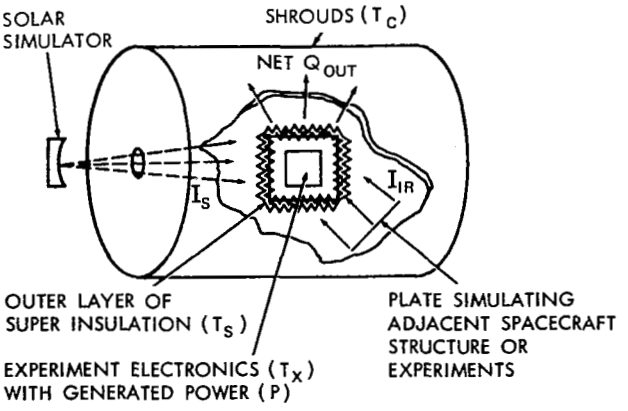

Figure 1—Typical test configuration for fully insulated experiment package.

In the subsequent discussion, the following assumptions are made:

1. The chamber shrouds form an isothermal heat sink that can be maintained at between -160°C and -190°C.
2. The chamber-wall emissivity is unity.
3. The experiment package is small relative to the shroud enclosure.
4. The experiment package is perfectly insulated against conductive losses resulting from mechanical attachment. This does not preclude conduction losses through the superinsulation.
5. All external surfaces of the superinsulation are "opaque."

The equation describing the steady-state heat transfer from the experiment electronics to the outer layer of superinsulation is:

$$P = \sum_{j=1}^{n} \sigma A_j \epsilon_{SI} \left[T_X^4 - (T_S)_j^4 \right]^* \tag{1}$$

$$\frac{P}{\epsilon_{SI}} = \sigma A_T T_X^4 - \sigma \sum_{j=1}^{n} A_j (T_S)_j^4 \tag{2}$$

The external experiment heat balance may be written (see Figure 1) as

$$P + Q_S + Q_{IR} = \sum_{j=1}^{n} \sigma A_j \epsilon_S \left[(T_S)_j^4 - T_C^4 \right] \tag{3}$$

$$P + \alpha_S A_S I_S + \alpha_{IR} A_{IR} I_{IR} = \sigma \epsilon_S \sum_{j=1}^{n} A_j \left[(T_S)_j^4 - T_C^4 \right] \tag{4}$$

which, rearranged, becomes

$$\frac{P}{\epsilon_S} + \frac{\alpha_S A_S I_S}{\epsilon_S} + \frac{\alpha_{IR} A_{IR} I_{IR}}{\epsilon_S} = \sigma \sum_{j=1}^{n} A_j \left[(T_S)_j^4 \right] - \sigma A_T T_C^4 . \tag{5}$$

*Symbols are listed in Appendix A.

Combining Equations 2 and 5 gives an overall heat balance equation between the experiment electronics and chamber shroud in the form:

$$\frac{P}{A_T}\left(\frac{1}{\epsilon_S}+\frac{1}{\epsilon_{SI}}\right)+\frac{\alpha_S A_S I_S}{\epsilon_S A_T}+\frac{\alpha_{IR} A_{IR} I_{IR}}{\epsilon_S A_T} = \left(\sigma T_X^4-\sigma T_C^4\right) . \tag{6}$$

Let

$$\epsilon^* = \frac{1}{\epsilon_S}+\frac{1}{\epsilon_{SI}} . \tag{7}$$

Substitution of Equation 7 in Equation 6 yields

$$\epsilon^* \frac{P}{A_T}+\frac{\alpha_S A_S I_S}{\epsilon_S A_T}+\frac{\alpha_{IR} A_{IR} I_{IR}}{\epsilon_S A_T} = \left(\sigma T_X^4-\sigma T_C^4\right) . \tag{8}$$

If there is no adjacent spacecraft structure experiment, or simulation of such, the IR energy input becomes zero. Thus Equation 8 reduces to

$$\epsilon^* \frac{P}{A_T}+\frac{\alpha_S A_S I_S}{\epsilon_S A_T} = \left(\sigma T_X^4-\sigma T_C^4\right) . \tag{9}$$

Similarly, if the simulated solar input is zero, Equation 9 is further simplified to

$$\epsilon^* \frac{P}{A_T} = \left(\sigma T_X^4-\sigma T_C^4\right) . \tag{10}$$

Analysis reveals that the energy difference between the experiment, σT_X^4, and the chamber wall, σT_C^4, is equated to the power dissipation multiplied by the effective emissivity ϵ^*. The emissivity, however, should more properly be considered a conductance parameter in the heat-transfer equation; that is, from Equation 10:

$$\frac{P}{A_T} = \frac{1}{\epsilon^*}\left(\sigma T_X^4-\sigma T_C^4\right) , \tag{11}$$

which is of the form

$$Q = C\Delta T = \frac{1}{R}\Delta T ,$$

where C is the conductance and R is the resistance. The point being made here is that the conductance parameter ϵ^* in Equation 11 is isolated in the equation; and this value, while presented above

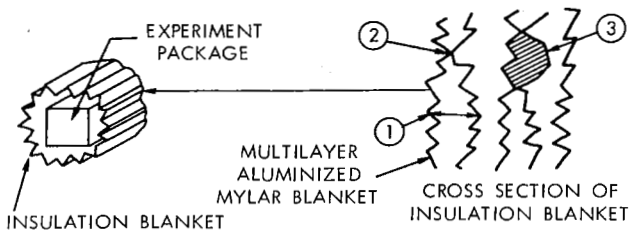

Figure 2—Aluminized Mylar experiment blanket.

simply as a radiation term, is in fact a function of the radiation and conduction through the superinsulation.

The heat transfer through the insulation (Figure 2) is brought about not only by radiation in area 1, but also by conduction in area 2, where the layers of insulation are touching, and by air conduction in area 3.

Because the influence of conduction (commonly referred to as "thermal shorts") influences the overall conductance value and varies between assemblies, the heat transfer equation is modified symbolically to

$$Z\left(\frac{P}{A_T}\right) = \left(\sigma T_X^4 - \sigma T_C^4\right) . \tag{12}$$

where Z, the effective transfer modulus, is a function of radiation and conduction;

$$Z = f\left(\epsilon^*, \frac{KA}{X}\right) ;$$

and, considering the solar and infrared input,

$$Z\left(\frac{P}{A_T}\right) + \frac{\alpha_S A_S I_S}{\epsilon_S A_T} + \frac{\alpha_{IR} A_{IR} I_{IR}}{\epsilon_s A_T} = \sigma T_x^4 - \sigma T_c^4 . \tag{13}$$

Equations 12 and 13 provide all the mathematical tools necessary to complete the simplified test approach. Equation 12 may be used to calculate Z using empirically obtained values of P, T_X, and T_C during an eclipse phase test.

The calculated value of Z, determined for the simpler eclipse phase test (Equation 12), and the magnitude of the solar input, may be substituted in Equation 13, thereby making it possible to solve for the experiment temperature T_X. The results may be used in lieu of a solar simulation test.

TEMPERATURE ANOMALY

Briefly, the OGO spacecraft (Figure 3) consists of a 6 × 3 × 6 main body, two solar arrays, and ten externally mounted experiments (designated EP's) located on the extremities of the different length booms.

Except for the solar array sides (+x and −x) and the +y face, which have temperature-actuated louvers, the thermal control of the mainbody is maintained by multilayered aluminized Mylar. All

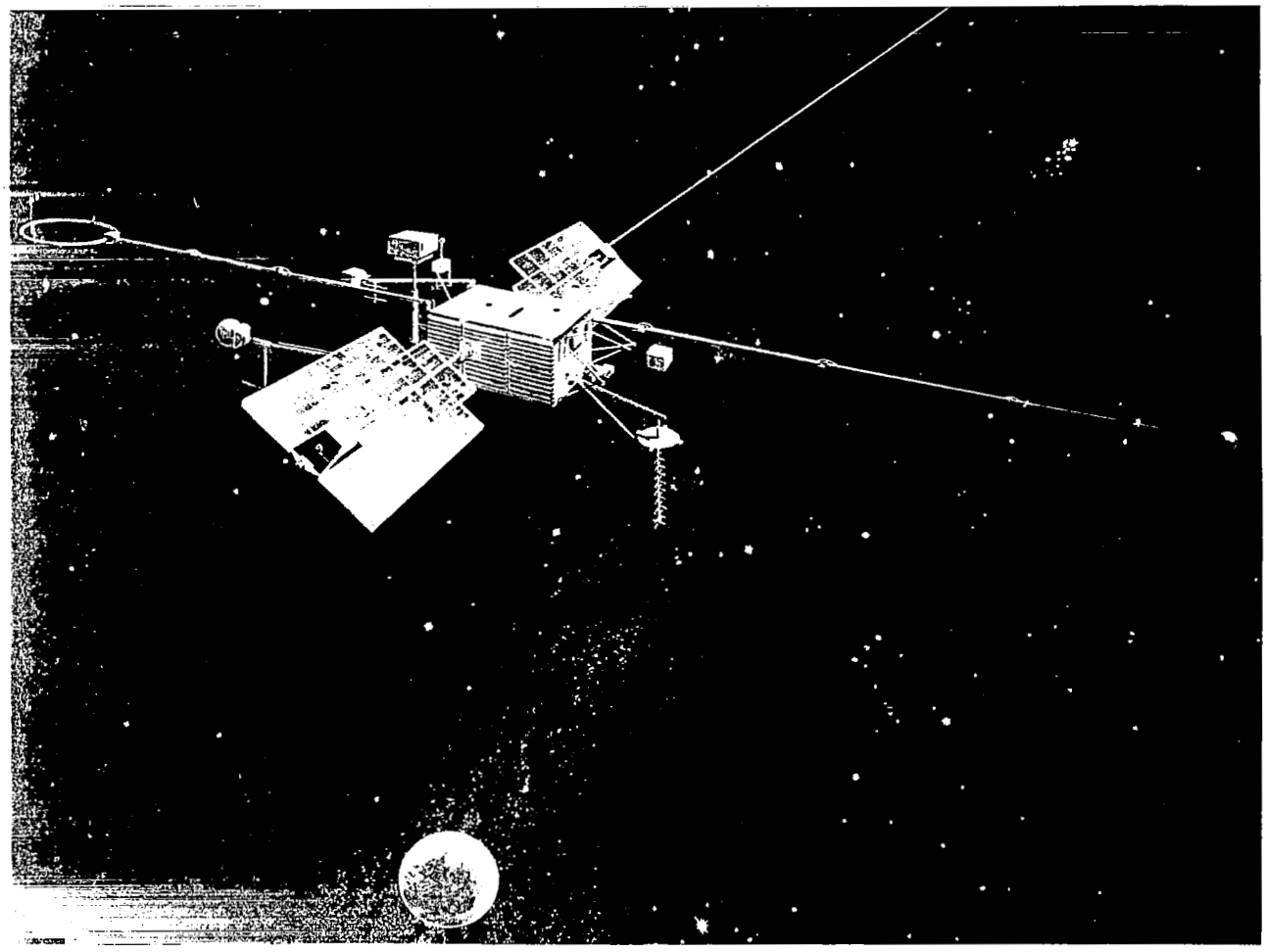

Figure 3—OGO III spacecraft.

the experiment packages can be considered as separate satellites, each requiring a separate design; their thermal controls are either passively designed (paint) or fully insulated.

To prove out the thermal adequacy of the design, the development test program for the OGO consisted of unit-level testing on all prototype and flight subsystems followed by a final integrated, or "all-up" test. Table 1 shows the results of the initial subsystem test and the later integrated spacecraft test on the insulated package, EP-1, during the OGO III test program that subsequently led to the technique development.

In order to account for the lack of agreement between temperatures found in the unit test and those found in the "all-up" test, a number of possibilities were considered. These include differences in the solar input, the possibility that the boom may have been exposed in one case and shaded in the other, and possible differences in solar-input spectra. However, none of these possibilities were determined to be sufficient reasons for the anomaly. It therefore became necessary to develop the chamber-shroud heat-balance equations already presented.

Table 1

OGO-B EP-1 Temperature Anomaly.

Test	Chamber	Simulator	IR Input	Stabilization Temperature	
				Solar (°C)	Eclipse (°C)
Unit level or subsystem	7 × 8*	Carbon-arc	(none simulated)	+23	(not run)
"All-up" or integrated spacecraft	SES*	Mercury-xenon	Solar array	+47	+24

*See Figure 4 for test configuration.

APPLICATION OF THE ANALYTICAL TECHNIQUE

The analysis was initially a diagnostic tool to determine which, if either, test results were correct. The study indicated that the anomaly existed partly because the subsystem test configuration did not include all the thermal inputs. As shown in Figure 4(a) the configuration of the subsystem

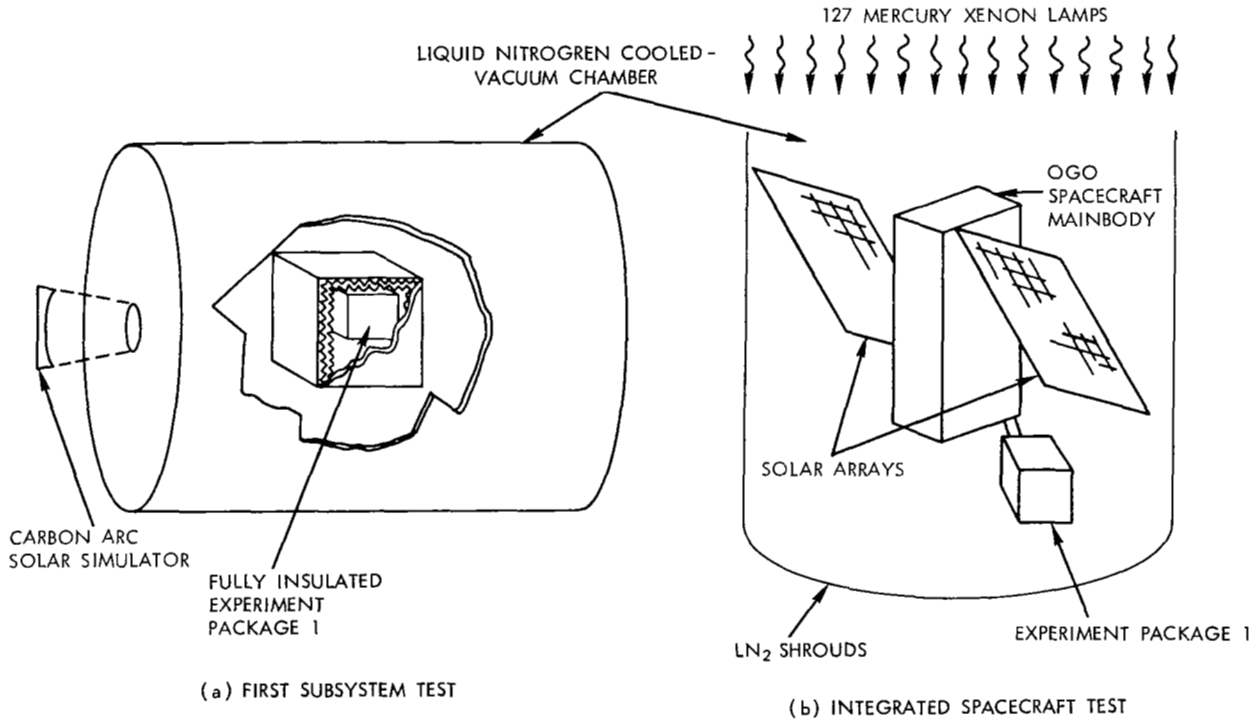

Figure 4—Unit vs. integrated test configurations.

test included only the cold-wall and solar-irradiation simulation. The solar-array infrared energy emission was neglected. In the system test—Figure 4(b)—the experiment package was exposed to the energy transfer from the solar array.

The subsystem was then removed from the spacecraft and reconfigured in the small vacuum facility; in this run the solar array was simulated by a small black plate. Table 2 shows that the results of this subsystem retest agree closely with the "all-up" spacecraft test findings.

Table 2

Comparison of Test Results.

Test	Experiment Temperature	
	Solar (T_x) (°C)	Eclipse (T_y) (°C)
Integrated spacecraft test	+47 (113°F)	+24 (75.2°F)
Subsystem retest	+44	+21

At this point, to illustrate how the technique was employed, an analysis will be made for the integrated spacecraft test. Substituting the data for the eclipse case (Tables 2 and 3) in Equation 12 gives

$$Z\left(\frac{P^*}{A_T}\right) = \left(\sigma T_X^4 - \sigma T_C^4\right) \cdots (12)$$

$$Z\,\frac{(15.36)}{(1.73)} = \sigma\left[(535.2)^4 - (204.0)^4\right]$$

or

$$Z = 15.49 \ .$$

Substituting this value in Equation 13, using the data from Table 3 for the solar case, yields

$$Z\left(\frac{P}{A_T}\right) + \frac{\alpha_S A_S I_S}{\epsilon_S A_T} + \frac{\alpha_{IR} A_{IR} I_{IR}}{\epsilon_S A_T} = \left(\sigma T_X^4 - \sigma T_C^4\right) \cdots (13)$$

$$15.49\left[\frac{4.0\times3.413}{1.73}\right]+\frac{0.25\times0.586\times123\times3.413}{0.75\times1.73}+\frac{14.5}{0.75\times1.73}=\sigma T_X^4-\sigma T_C^4$$

$$122.24+47.39+11.18=\sigma\left[T_X^4-(204.0)^4\right]$$

i.e.,

$$T_X = 112°F \text{ (or } 44.4°C) .$$

This calculated value evidently is in fair agreement with the test value: 47°C.

Table 3

Conditions Surrounding the Test.

Shroud temperature (T_C)	-160°C (-256°F)
Experiment heat dissipation-solar (P)	4.0 watts = 13.65 Btu/hr
Experiment heat dissipation-eclipse (P)	4.5 watts = 15.36 Btu/hr
Solar simulator intensity (I)	123 watts/ft^2
Absorbed IR intensity α_{IR} A_{IR} ($F\epsilon\sigma T^4$)	14.5 Btu/hr
Where: Form factor (F)	0.17
Array temp. (T)	+149°F
Array emissivity (ϵ)	0.8
Emissivity AL-Mylar $(\epsilon)_s$ (Mylar side out)	0.75
Solar absorptivity AL-Mylar (α_s)	0.25
IR absorptivity AL-Mylar (α_{IR}) (Mylar side out)	0.75
Areas:	
Total	1.73 feet^2
Solar absorbing	0.586 feet^2
Infrared absorbing	0.586 feet^2

REVISED TEST APPROACH

The success realized in the EP-1 temperature anomaly situation caused a reexamination of the test technique used on unit-level testing of all fully insulated packages.

The standard program (Figure 5, Technique A) consists of two separate solar and eclipse tests with temperature stabilization comparisons made between the prototype-model and flight-model test results. The revised approach (Technique B) reduces the testing to a solar and eclipse run on the prototype and a single thermal-vacuum test on the flight model. In addition, the revised technique combines the environmental testing with analytical validation of the test results.

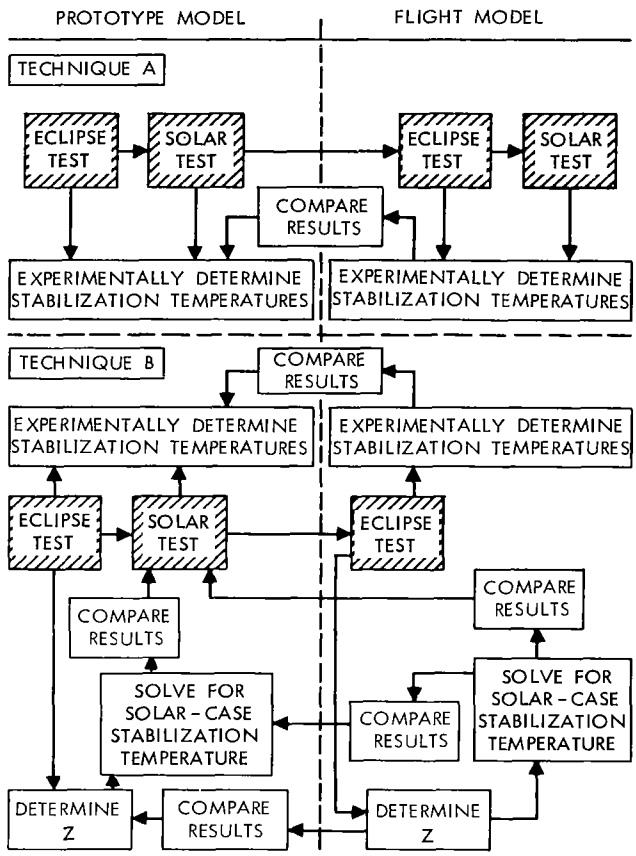

Figure 5—Diagramatical comparison of standard and revised test approach for prototype and flight models.

Since solar simulation is several times more complicated and time-consuming than thermal-vacuum testing, the reduction of effort and time is not merely 25 percent (that is, one test phase out of a total of four) but possibly closer to 40 percent, when the whole program is considered.

The standard test approach is straightforward. The tests are performed and the temperature stabilizations of models compared. Since aluminized mylar blankets are manually assembled and therefore subject to compression and thermal shorts, the prototype and flight models often have different temperature stabilizations. If the differences are small and the temperatures within the allowable operating range, the flight-unit thermal design was considered acceptable. A large temperature difference, however, was considered cause for rejection.

The revised test approach begins with a solar and eclipse test on the prototype experiment. Coincident with eclipse phase testing, the effective transfer modulus, z, is determined and the solar stabilization temperature predicted by the analytical technique. The empirically obtained value is compared with the predicted value in order to validate test conditions and technique applicability. When the flight model is subjected to environmental conditions, the eclipse test is performed as part of the thermal-vacuum performance test. As before, the effective transfer modulus is determined and the solar-phase temperature stabilization is calculated. Comparisons are then made between prototype and flight models, for the effective transfer modulus and for the stabilization temperature. If there are discrepancies (in spite of the mechanical design and heat dissipation rate of the electronics not being altered between the prototype and flight models), it is concluded that the effectiveness of the insulation blanket is different from that of the verified prototype-design blanket. As in the standard test approach, a significant difference would be cause for making the solar test, rejecting the design, or both.

VERIFICATION OF TECHNIQUE

The next OGO spacecraft to undergo development testing was the OGO-E; two fully insulated assemblies were included in the complement of experiments. Since technique B (Figure 5) still required verification, it was necessary to perform the solar test on the flight model; the calculated temperature was then compared with the empirical value. The results follow:

	Flight Model Solar Case Stabilization Temperatures °C	
Experiment	Calculated	Empirical
EP-1	13.0	17
EP-3	11.7	13

On the basis of these results, in addition to the OGO-III EP-1 study, the technique B (Figure 5) was incorporated in the standard testing procedures and will be employed in the future.

LIMITATIONS OF THE REVISED TEST APPROACH

The combined test-analytical techniques are at present limited to specific types of assembly having the following characteristics:

1. The experiment package must be fully insulated with at least five layers of aluminized mylar.
2. The experiment flight conditions must include both solar and eclipse phases.
3. The heat dissipation rate of the experiment electronics must be small. (The highest heat rate for the OGO experiments was in the 5-watt range.)
4. The internal structure of the experiment must be of a metal such as aluminum. The structure or experiment baseplate must be metallic, so that the temperature gradient is small. (If the gradient is large, the location of the reference thermocouple is critical and a significant error may result.)
5. Regardless of the baseplate material, the reference thermocouple should always be located in the same general area on the prototype and flight models.

Another condition that affects the baseplate gradient, and thus limits the extensive use of the revised test approach at present, is the presence of sensor openings in the insulation blanket. Certainly the size of the opening dictates the magnitude of the gradient, but it appears probable that packages with small openings could be tested without seriously compromising the validity of the test approach. More experimental experience is required, however, to determine the maximum openings that may be tolerated.

ACKNOWLEDGMENT

The author wishes to acknowledge the editorial and technical review by Messrs. A. L. Seivold, W. Auer, and H. Mauer, Jr.

Goddard Space Flight Center
National Aeronautics and Space Administration
Greenbelt, Maryland, April 2, 1968
697-06-01-14-51

BIBLIOGRAPHY

Chapman, A. J., "Heat Transfer," Second edition, New York: MacMillan, 1967.

Jacob, M., "Heat Transfer," Volume II, New York: John Wiley, 1957.

McAdams, W. H., "Heat Transmission," Third edition, New York: McGraw-Hill, 1954.

Appendix A

List of Symbols

A_j j^{th} area of external surface of superinsulation

A_{IR} area of package irradiated by infrared inputs

A_S projected area of package irradiated by solar beam

A_T total area of external surface of superinsulation

I_R intensity of infrared inputs

I_S solar intensity at plane of the package

KA conductivity times area

P internal heat generation of experiment

Q_{IR} total infrared input to package

Q_S total solar heat input to package

T_C absolute temperature of chamber shrouds

$(T_S)_j$ absolute temperature of j^{th} area of external surface of superinsulation

T_X absolute temperature of experiment electronics

Z effective transfer modulus, i.e., function of radiation and conduction = $f(\epsilon^*, KA)$

α_{IR} package-surface infrared absorptivity

α_S package-surface solar absorptivity

ϵ_S emissivity of external surface of superinsulation

ϵ_{SI} effective emissivity through layers of superinsulation

ϵ^* $\frac{1}{\epsilon_S} + \frac{1}{\epsilon_{SI}}$

σ Stefan-Boltzmann constant